RESEARCH PAPER

Formulation and Evaluation of Mouth Dissolving Tablet Containing Aprepitant for Chemotherapy Induced Nausea and Vomiting

Choudhari Kanchan[1*], Shinde Jitendra [2], Bhosale Ashok[3]

[1]Department of Pharmaceutics, Shankarrao Ursal College of Pharmaceutical Sciences and Research Centre, Kharadi Pune,Maharashtra, India

Email: choudharikanchan14@gmail.com

[2]Head of Department of Pharmaceutics, Shankarrao Ursal College of Pharmaceutical Sciences and Research Centre, Kharadi Pune,Maharashtra, India

[3]Principle, Shankarrao Ursal College of Pharmaceutical Sciences and Research Centre, Kharadi Pune,Maharashtra, India

ABSTRACT

Objectives: Aprepitant is a poorly soluble BCS Class IV NK_1 receptor antagonist that causes chemotherapy-induced nausea and vomiting (CINV). The purpose of this research was to develop and optimize Aprepitant mouth dissolving tablets (MDTs) to improve its dissolution and compliance, especially in cancer patients with dysphagia.

Methods: Preformulation studies such as solubility, FTIR, and DSC were conducted to understand the drug-excipient compatibility. A 3^2 full factorial design was used to optimize the formulations (KF1-KF9) of MDTs, considering Kollidon® VA64 (A) and Crospovidone XL-10 (B) as independent variables and disintegration time (Y_1) and in vitro drug release after 15 min (Y_2) as responses. Following direct compression, tablets were tested for pre- and post-compression features, dissolution (PBS pH 6.8) and accelerated stability (40 ± 2 °C / 75 ± 5% RH, 90 days).

Results: Powder blends showed good flowability (Carr's index < 13.5%). All batches had post-compression parameters within pharmacopoeial limits. Quadratic polynomial was the optimal model for both responses (R^2 = 0.9982 for Y_1; R^2 = 0.9991 for Y_2). Kollidon® VA64 had the greatest impact on both responses. Batch KF9 with the highest excipient concentrations was identified as the optimal formulation due to the shortest disintegration time (37.2 sec), highest Q_{15} (93.4 ± 2.6%) and almost complete drug release (99.3 ± 2.9%) within 45 min. Stability tests revealed no significant drug loss (98.63 ± 0.74%) or change in dissolution for up to 90 days.

Conclusion: The KF9 formulation had short disintegration time and enhanced dissolution, providing clinically relevant benefits for CINV treatment in dysphagia patients. These results suggest the clinical feasibility of developing Aprepitant MDTs and its in vivo pharmacokinetics should be evaluated.

Keywords: Aprepitant; mouth dissolving tablets; Kollidon® VA64; Crospovidone XL-10; factorial design; dissolution enhancement.

How to cite this article: Kanchan C, Jitendra S, Ashok B. Formulation and Evaluation of Mouth Dissolving Tablet Containing Aprepitant for Chemotherapy Induced Nausea and Vomiting. Int J Drug Deliv Technol. 2026;16(63s):885.902 DOI: 10.25258/ijddt.16.63s.87

INTRODUCTION

Nausea and vomiting induced by chemotherapy (CINV) continues to be one of the most distressing and common side effects experienced by cancer patients receiving treatment. Cancer is a major source of morbidity and mortality worldwide, with more than 19 million new cancers reported each year [1]. CINV is reported in 70-80% of patients treated with moderately to highly emetogenic chemotherapy in the absence of, or due to suboptimal management of, antiemetic prophylaxis [2]. The syndrome negatively affects quality of life, impairs treatment adherence and leads to unexpected hospital admissions, thus increasing the financial health-care burden globally [3]. The estimated cost burden associated with CINV globally is in the billions of dollars annually, both in direct and indirect costs, and places significant financial burdens on individuals and institutions. Current antiemetic approaches, such as $5\text{-}HT_3$ receptor antagonists and steroids, are ineffective in tackling delayed CINV, which occurs 24-120 hours after chemotherapy [4]. Moreover, the oral solid forms of currently available antiemetics pose difficulties due to dysphagia, low patient compliance (especially in frail cancer patients), and unpredictable absorption from the gastrointestinal tract. These continuing challenges highlight the critical need for new, patient-friendly approaches to drug delivery that more effectively combat CINV [5].

The potent and selective neurokinin-1 (NK_1) receptor antagonist Aprepitant has become a key anti-emetic in the prevention of both acute and delayed CINV. Also known as 5-[[(2R,3S)-2-[(1R)-1-[3,5-bis(trifluoromethyl)phenyl]ethoxy]-3-(4-fluorophenyl)-4-morpholinyl]methyl]-1,2-dihydro-3H-1,2,4-triazol-3-one,

Aprepitant is highly lipophilic (log P ≈ 5.0), poorly soluble in water (BCS Class IV), with an oral bioavailability of 59-67% due to significant first-pass metabolism by CYP3A4 [6]. The drug competitively inhibits binding of substance P at central and peripheral NK_1 receptors found in the vomiting centre and gastrointestinal tract, thus blocking the emetic signalling pathway triggered by cytotoxic drugs [7] .The potent antiemetic efficacy of Aprepitant compared to conventional 5-HT_3 antagonists has been consistently demonstrated in preclinical and clinical studies for complete response in acute and delayed phases of CINV [8]. But its poor physicochemical characteristics such as poor wettability, hydrophobicity and dissolution-dependent absorption require novel formulation strategies to improve its bioavailability and achieve plasma therapeutic levels upon oral administration [8].

Mouth dissolving tablets (MDTs) are a technologically advanced oral solid dosage form that rapidly disintegrates in the mouth (within 60 seconds) in the presence of saliva, eliminating the need for water. This feature makes MDTs particularly suitable for elderly, paediatric and cancer patients who often suffer from dysphagia, nausea, or weakness [9]. The fast disintegration of MDTs enables pre-gastric absorption through the buccal and sublingual routes, thus bypassing first-pass hepatic metabolism, and potentially enhancing drug bioavailability [10]. The choice of superdisintegrants (e.g. crospovidone, sodium starch glycolate, and croscarmellose sodium), diluents and flavours determine the disintegration profile and palatability of MDTs. Recent developments in direct compression and sublimation technologies have also facilitated MDT production while maintaining tablet strength [11]. The use of MDT technology for enhancing the oral delivery of BCS Class IV drugs such as Aprepitant, therefore, offers a scientifically sound and clinically relevant approach to overcoming current bioavailability and compliance issues [12].

The current study intends to develop and optimise mouth dissolving tablets of Aprepitant via design-of-experiment-based approaches, with the main goal of improved dissolution and compliance. The secondary objectives include physicochemical characterization, in vitro drug release studies and accelerated stability studies according to ICH Q1A(R2) guidelines, which, in turn, justify the therapeutic promise of the optimized formulation in the treatment of CINV.

MATERIALS AND METHODS

Materials

Aprepitant (pharmaceutical grade, purity ≥ 99.5%, MW 534.43 g/mol) was procured from Sciquaint Innovations Pvt. Ltd., Pune, India. Kollidon® VA64 (pharmaceutical grade, vinylpyrrolidone-vinyl acetate copolymer, viscosity 25-35 mPa·s) and Crospovidone XL-10 (USP/NF grade, cross-linked polyvinylpyrrolidone, particle size ≤ 50 µm) were procured from Sciquaint Chemicals, Pune, India. Microcrystalline cellulose PH 102 (NF grade, particle size 100 µm) and mannitol (USP grade, directly compressible grade) were procured from Research Lab Fine Chem Industries, Mumbai, India. Magnesium stearate (BP grade, lubricant grade) and talc (IP grade, purified) were obtained from Research Lab Fine Chem Industries, Mumbai, India. Potassium dihydrogen phosphate and disodium hydrogen phosphate (for preparation of phosphate buffer saline pH 6.8) were procured from Research Lab Fine Chem Industries, Mumbai, India. Methanol, acetone, ethanol and dimethyl sulfoxide (DMSO) of analytical grade were obtained from Research Lab Fine Chem Industries, Mumbai, India. Hydrochloric acid (analytical grade) required for preparation of 0.1 N HCl solution was procured from Research Lab Fine Chem Industries, Mumbai, India. Other chemicals and reagents used were of analytical grade obtained from commercial sources.

METHODS

Calibration Curve of Aprepitant

A calibration curve was developed and used to calculate the Aprepitant concentrations in all analytical studies. A stock solution of Aprepitant (1 mg/mL) was prepared by dissolving 10 mg of accurately weighed Aprepitant in 10 mL of methanol (Research Lab Fine Chem Industries, Mumbai, India). The solution was serially diluted with phosphate buffer saline (PBS) pH 6.8 to prepare the working concentrations of 2, 4, 6, 8, 10, 12, 14 and 16 µg/mL. The absorbance was measured at λmax 264 nm using a UV-Vis spectrophotometer. PBS pH 6.8 was used as a blank. The Beer-Lambert law was validated and the calibration curve was drawn as a plot of absorbance vs concentration. The coefficient of determination (R^2) was used to determine linearity. Triplicate readings (n = 3) were taken and results reported as mean ± SD [13,14].

FTIR Analysis

Fourier transform infrared spectrometry (FTIR) was used to detect functional groups of Aprepitant and to evaluate any physical and chemical interactions between drug and excipients in the physical mixture. About 2 mg of pure Aprepitant and the physical mixture (Aprepitant: Kollidon® VA64: Crospovidone XL-10 in ratio corresponding to formulation composition) were mixed with IR-grade potassium bromide (KBr) at a ratio of 1:100 (w/w) and KBr pellets were prepared by pressing the powder mixture in a hydraulic KBr press at 10 tonnes for 2 min. Spectra were obtained using an FTIR spectrophotometer in the wavenumber range from 4000-400 cm^{-1} at 4 cm^{-1} resolution, scanning 32 times. The comparison of pure Aprepitant and physical mixture spectra was made to ascertain the presence or shift of characteristic bands. Triplicate measurements (n = 3) were made [15,16].

DSC Analysis

DSC analysis was carried out to assess the thermal characteristic of Aprepitant and to determine any thermal interactions and/or changes in crystallinity state in the physical mixture with excipients. Accurately weighed amounts (5 ± 0.5 mg) of pure Aprepitant and a physical mixture were loaded into sealed aluminum pans. DSC thermograms were obtained using a differential scanning

calorimeter (DSC 60 Plus, Shimadzu India Pvt. Ltd., Bengaluru, India) at a scan rate of 10 °C/min from 30-300 °C under a flow of nitrogen (30 mL/min). An empty sealed aluminum pan was used as the reference. The onset of the melting endotherm and the enthalpy of fusion (ΔH, J/g) were measured. Preservation or loss of the Aprepitant endothermic peak in the physical mixture was considered as compatibility or interaction, respectively. The studies were carried out in triplicate (n = 3) [17].

Solubility Study

Preformulation solubility profiling of Aprepitant was performed in different solvents. Aprepitant (excess) was added to 10 mL each of distilled water, phosphate buffer pH 6.8, phosphate buffer pH 7.4, 0.1 N HCl, and methanol in tightly sealed vials. The vials were kept in a thermostated orbital shaker and shaken at 25 ± 0.5 °C at 100 rpm for 72 h for equilibrium solubility. Aliquots were filtered through a 0.45 µm nylon membrane filter (Neeta Chemicals, Pune, India), suitably diluted with the same medium and the absorbance was measured at 210 nm on the UV-Vis spectrophotometer mentioned in Section 2.1. Concentration of drug was calculated from the standard curve. All experiments were carried out in triplicates (n = 3) and the results reported as mean ± SD (µg/mL) [18,19].

Experimental Design

The effect of two independent variables on the properties of Aprepitant mouth dissolving tablet (MDTs) was studied using a 3^2 full factorial design. The factors were: X1, concentration of Kollidon® VA64 (vinylpyrrolidone-vinyl acetate copolymer; BASF Corp., Germany), a new excipient that has not previously been used as a functional disintegrant-enhancing polymer in Aprepitant MDTs and X2, concentration of Crospovidone (Polyplasdone XL-10; Ashland Inc., USA), a common crosslinked superdisintegrant. Three levels of each factor were investigated: low (-1), medium (0) and high (+1). The responses (dependent variables) were: Y1, disintegration time (DT in seconds) with a goal of minimum, and Y2, cumulative percentage drug release at 15 min (Q_{15}, %) with a goal of maximum. Nine formulations (F1-F9) were obtained from the 3^2 factorial design. The general response polynomial equation is:

$$Y = b_0 + b_1X1 + b_2X2 + b_{12}X1X2 + b_{11}X1^2 + b_{22}X2^2$$

where Y is the measured response (Y1 or Y2), b_0 is the intercept, b_1 and b_2 are the coefficients for the main effects of Kollidon® VA64 and Crospovidone XL-10, b_{12} is the interaction coefficient, and b_{11}, b_{22} are the quadratic coefficients. Design-Expert® software (v13.0, Stat-Ease Inc., USA) was used for design generation, coefficient estimation, ANOVA, and graphical analysis of response surface plots [20,21].

Table 1: Independent and Dependent Variables for 3^2 Full Factorial Design

Variable	Type	Low (−1)	Medium (0)	High (+1)
X1: Kollidon® VA64 (mg/tablet)	Independent	10	20	30
X2: Crospovidone XL-10 (mg/tablet)	Independent	4	8	12
Y1: Disintegration Time (sec)	Dependent	-	-	Minimize
Y2: Cumulative drug release at 15 min (%)	Dependent	-	-	Maximize

Table 2: Formulation Table for Aprepitant MDTs (KF1-KF9) per Tablet (300 mg)

Ingredient	KF1	KF2	KF3	KF4	KF5	KF6	KF7	KF8	KF9
Aprepitant (mg)	80	80	80	80	80	80	80	80	80
Kollidon® VA64 (mg)	10	20	30	10	20	30	10	20	30
Crospovidone XL-10 (mg)	4	4	4	8	8	8	12	12	12
Mannitol DC (mg)	148	144	140	138	134	130	128	124	120
Microcrystalline Cellulose PH 102 (mg)	40	40	40	40	40	40	40	40	40
Aspartame (mg)	5	5	5	5	5	5	5	5	5
Magnesium Stearate (mg)	3	3	3	3	3	3	3	3	3
Aerosil 200 (mg)	2	2	2	2	2	2	2	2	2
Peppermint flavor (mg)	8	8	8	8	8	8	8	8	8
Total (mg)	300	300	300	300	300	300	300	300	300

Preparation of Aprepitant Mouth Dissolving Tablets

Aprepitant MDTs (KF1-KF9) were manufactured using direct compression. All ingredients were separately screened through sieve #60 (250 µm) and dried at 40 °C for 30 min before mixing. Aprepitant (80 mg) was geometrically mixed with Kollidon® VA64 and Crospovidone XL-10 as per Table 2 followed by addition of mannitol DC (Pearlitol 200SD) and MCC PH 102 and continued mixing for 10 min using a laboratory-scale blender (V-cone blender, Electrolab, Mumbai, India). Aerosil 200 (colloidal silicon dioxide) was added as a glidant and blended for 5 min followed by aspartame and peppermint flavor. Pre-screened (sieve #60) magnesium stearate was added as a lubricant and blended for 2 min. The powder blend was compressed into a 300 mg target weight tablet using a 10-station rotary tablet machine (Rimek Mini Press-II, Karnavati Engineering Ltd., India) using 10 mm round flat-faced punches at a compression pressure of 5-7 kN. The blend was characterized for pre-compression attributes (angle of repose, bulk density, tapped density,

Carr's index, Hausner's ratio) before compression [22].

Characterization of Aprepitant Mouth Dissolving Tablets

Pre-Compression Evaluation

Angle of Repose

The angle of repose of the powder blend was measured to evaluate the flow properties of the powder blend/granules before compression. The powder blend was slowly poured through a funnel set at a height of 10 cm above a horizontal surface and a cone of powder was formed. The radius (r) and height (h) of the cone were measured and the angle of repose (θ) was determined by the equation:

$\tan \theta = h / r$

The powder blends with angle of repose ≤ 30° were classified as having good flowability, while between 31-35° were classified as having fair flowability, according to the pharmacopeial classification. Triplicate samples (n = 3) were studied and the results were reported as mean ± SD [23].

Bulk Density

Bulk density of the various formulation blends (KF1-KF9) was measured by filling a 100 mL graduated glass measuring cylinder, without tapping, with a pre-weighed amount of powder (W). The volume of powder (Vbulk) was measured and bulk density was calculated as:

Bulk Density (g/mL) = W / Vbulk

Measurements were performed in triplicate (n = 3) and results expressed as mean ± SD in g/mL [24].

Tapped Density

Tapped density was determined using a tap density tester (Electrolab ETD-1020, Electrolab India Pvt. Ltd., Mumbai, India). The same powder sample used for bulk density determination was subjected to mechanical tapping at a rate of 300 taps/min. The tapped volume (Vtapped) was recorded after 500 taps, and tapped density was calculated as:

Tapped Density (g/mL) = W / Vtapped

All measurements were performed in triplicate (n = 3) and expressed as mean ± SD [25].

Carr's Compressibility Index

Carr's compressibility index (CI) was calculated from the bulk and tapped density values as an indirect measure of powder compressibility and flowability using the following equation:

CI (%) = [(Tapped Density − Bulk Density) / Tapped Density] × 100

Values of CI ≤ 15% were interpreted as excellent compressibility, 16–20% as good, and ≥ 26% as poor compressibility, as per USP classification. All calculations were performed in triplicate (n = 3) [26].

Hausner's Ratio

Hausner's ratio was calculated from bulk and tapped density values as an additional indicator of powder flow and interparticulate friction using the equation:

Hausner's Ratio = Tapped Density / Bulk Density

A Hausner's ratio of < 1.25 indicates good flow, while values > 1.25 indicate poor flowability. All measurements were carried out in triplicate (n = 3) and results expressed as mean ± SD [27].

Post-Compression Evaluation

Tablet Appearance and Organoleptic Evaluation

The tablets of all formulations (KF1-KF9) were examined visually for surface appearance, colour, capping, lamination, chipping or other physical defects. The organoleptic evaluation also included shape, colour, odour and taste of tablets. At least 20 tablets of each batch (KF1–KF9) were visually inspected for any physical defects under sufficient light. Tablet Thickness and Diameter [28].

Tablet Thickness and Diameter

The thickness and diameter of ten tablets from each batch (KF1-KF9) were measured individually using a digital Vernier caliper (Mitutoyo Corporation, Japan) having least count 0.01 mm. Tablets were measured at the centre of the tablet face. The results were expressed as mean ± SD in mm (n = 10). Thickness uniformity is important for packaging, filling into blister and for appearance [29].

Hardness

Hardness, as a measure of tablet strength, was evaluated using a tablet hardness tester (Electrolab EH-01P, Electrolab India Pvt. Ltd., Mumbai, India). Six tablets from each batch were each placed between the two anvils of the tester and the load required to fracture the tablets diametrically was measured. The results were reported in kg/cm² as mean ± SD (n = 6). Hardness for MDTs is usually between 2-4 kg/cm² to provide sufficient mechanical strength and allow for quick disintegration [30,31].

Friability

Friability of tablets was evaluated by using a friabilator (Electrolab EF-2, Electrolab India Pvt. Ltd., Mumbai, India) to assess the resistance of tablets to mechanical shocks during manufacturing, packaging and shipping. A total of 20 tablets were weighed and rotated 100 times at 25 rpm for 4 min. The drum was carefully brushed to remove dust from the tablets before weighing again. % Friability was determined using the formula:

$\%\ \text{Friability} = [(W_0 - W) / W_0] \times 100$

where W_0 = weight of tablets before rotation test; W = weight of tablets after rotation. The acceptable friability value is ≤ 1.0% as per USP <1217>. All experiments were done in triplicate (n = 3) [32][33].

Weight Variation

Dose consistency (uniformity) was measured by weight variation. A sample of 20 tablets from each batch (KF1-KF9) were weighed individually with an analytical balance (Shimadzu AUW120D, Shimadzu India Pvt. Ltd., Bengaluru, India) and the average weight was determined. The weight of each tablet was compared to the mean weight, and the percentage deviation was determined for each tablet. The test was assessed as per the USP standard, which allows

up to ±7.5% deviation from the average weight for tablets weighing 200-300 mg. The data were reported as mean weight ± SD (n = 20) [34].

Drug Content Uniformity

Drug content uniformity was done to ensure the required quantity of Aprepitant was present in each tablet. Ten tablets of each batch (KF1-KF9) were powdered individually and exactly weighed powder of 80 mg Aprepitant was taken in a 100 mL volumetric flask. The powder was dissolved in 10 mL methanol, sonicated for 30 min using an ultrasonicator,(Labline Stock Centre Mumbai, India), volume made up to 100 mL with phosphate buffer (pH 6.8) and filtered through a 0.45 µm nylon membrane filter. It was further diluted and the absorbance was measured at 264 nm by a UV-Vis spectrophotometer (Jasco V-730 Spectrophotometer, Japan). The drug content was determined from the calibration curve and expressed as percentage of label claim (n = 10). The range is 90-110% as per USP [35].

Disintegration Time

In vitro disintegration time was measured using a tablet disintegration test apparatus (Electrolab ED-2L, Electrolab India Pvt. Ltd., Mumbai, India) with 6-tube assembly. Water (distilled) at 37 ± 0.5 °C was used as the disintegration medium as per IP/USP monograph for orally disintegrating tablets. A single tablet was placed in each tube of the basket, and the disintegration tester was started. The time from the tablet's placement in the apparatus to the time when it disintegrated, with no remnant left on the mesh screen other than starch granules and coating fragments, was considered as disintegration time. In the case of MDTs, a disintegration time of ≤ 30 seconds is acceptable according to the pharmacopeia. Six tablets (n = 6) were measured per batch, and results reported as mean ± SD (seconds) [36].

Wetting Time and Water Absorption Ratio

Wetting time and water absorption ratio (WAR) were measured as representative parameters for the hydrophilicity and porosity of the tablet matrix, which are in turn related to the disintegration and dissolution of MDTs. A 1 cm × 1 cm piece of tissue paper (folded twice) was immersed in a 10 mL Petri dish of distilled water containing Amaranth dye (0.1% w/v). After that one tablet was gently placed at the centre of wetted tissue paper without any external force and the time taken for the upper surface of the tablet to be wetted completely, as indicated by the uniform distribution of dye through the tablet, was measured as wetting time with a stopwatch. As soon as the tablet was fully wetted, it was removed, surface water was absorbed using tissue paper, and the tablet was weighed again. Water absorption ratio (R) was calculated using the following equation:

$$\mathbf{R = [(W_a - W_0) / W_0] \times 100}$$

Where W_a = weight of tablet after wetting and W_0 = weight of tablet before wetting. The measurements were carried out in triplicate (n = 3) and the results presented as mean ± SD [37].

***In Vitro* Drug Release**

The in vitro release of Aprepitant from MDTs (KF1-9) was determined by the USP Type II (paddle) apparatus (Electrolab TDT-08L, Electrolab India Pvt. Ltd., Mumbai, India). Phosphate buffer saline (PBS) pH 6.8 as dissolution medium was used at a temperature of 37 ± 0.5 °C and a paddle speed of 50 rpm. A single tablet was immersed in the dissolution medium in each vessel at the start of the study. Samples of 5 mL were withdrawn at predetermined time points of 2, 5, 10, 15, 20, 30 and 45 min and replaced with freshly prepared dissolution medium at the same temperature to ensure sink conditions. The withdrawn samples were filtered through a 0.45 µm nylon membrane filter, diluted with PBS pH 6.8 as required and the absorbance was measured at 264 nm in a UV-Vis spectrophotometer (Jasco V-730 Spectrophotometer, Japan). The cumulative percentage drug release was determined using the calibration curve. The drug release data were fitted to zero-order, first-order, Higuchi, and Korsmeyer-Peppas models, and the model with the highest coefficient of determination (R^2) was deemed to fit the data best. The release exponent n ($M_t/M_\infty = Ktn$) was determined from the Korsmeyer-Peppas model to determine the release mechanism: $n \leq 0.45$ suggests Fickian diffusion, $0.45 < n < 0.89$ suggests anomalous (non-Fickian) diffusion and $n \geq 0.89$ suggests Case-II transport. Dissolution experiments were conducted in triplicate (n = 3) and results presented as mean ± SD [38].

***In Vitro* Dispersion Time**

In vitro dispersion time was evaluated in a separate test from disintegration to determine how long it took for a tablet to completely disperse and form a uniform suspension when placed in a small volume of medium (simulating the oral cavity). A single tablet was added to a 10 mL beaker containing 2 mL of distilled water at 37 ± 0.5 °C, and the time taken for the tablet to completely disperse and form a homogeneous suspension without visible aggregates was measured. Triplicate measurements (n = 3) were made and the results were reported as mean ± SD in seconds. This is an important consideration in MDT performance where quick oral dispersion for convenience and ease of use is required [39].

Surface pH Measurement

The pH of the surface of the prepared MDTs was determined to predict mucosal irritation after oral administration. The tablet was swollen for 2 min by placing it on a flat surface in contact with 0.5 mL of distilled water. The pH of the swollen tablet surface was measured by putting the flat surface pH electrode (Lab India, Mumbai) in contact with the swollen tablet surface. The pH of the surface was measured. Triplicate measurements (n = 3) were taken and the results are presented as mean ± SD. The surface pH of a tablet should be in the range of 6.5-8.0 for compatibility with human oral mucosa [40].

RESULTS AND DISCUSSION

Results

Calibration curve determination

For Aprepitant, a calibration curve was prepared in phosphate buffer saline (PBS) pH 6.8 at the desired concentrations. It was described by the equation y = 0.0431x + 0.0014 and R^2 of 0.9999, indicating a linear dependence of absorbance on concentration. The UV spectrum in PBS pH 6.8 showed a λmax of 264 nm (Fig. 1) used for all spectrophotometric studies.

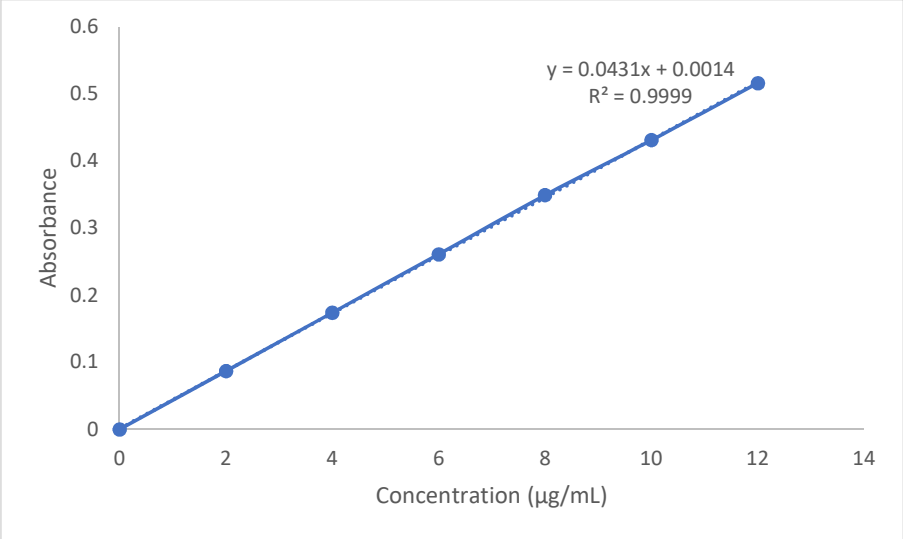

Figure 1: UV absorption spectrum of Aprepitant in PBS pH 6.8 showing λ_{max} at 264 nm.

Solubility profile of Aprepitant

The solubility profile of Aprepitant in different solvents and aqueous solutions (25 ± 0.5°C) is shown in Table 3. Aprepitant had low solubility in water, with values of 4.18 ± 0.21 µg/mL and 5.32 ± 0.34 µg/mL in distilled water and 0.1 N HCl (pH 1.2), respectively, considered as slightly soluble according to IP/USP guidelines. There was a slight increase in solubilities in phosphate buffer pH 6.8 (18.74 ± 0.62 µg/mL) and pH 7.4 (14.53 ± 0.47 µg/mL), which were classified as sparingly soluble. On the other hand, improved solubility was observed in organic solvents, with the highest value in DMSO (612.45 ± 9.73 µg/mL), followed by methanol (483.60 ± 8.12 µg/mL), ethanol (78.42 ± 2.09 µg/mL) and acetone (52.37 ± 1.84 µg/mL), exhibiting freely soluble or soluble properties. This data confirmed the lipophilic behaviour of Aprepitant and hence, its classification as a BCS Class IV drug.

Table 3. Solubility profile of Aprepitant in various solvents and aqueous media at 25 ± 0.5 °C

Solvent / Medium	Solubility (µg/mL)	Classification (IP/USP)
Distilled water	4.18 ± 0.21	Slightly Soluble
0.1 N HCl (pH 1.2)	5.32 ± 0.34	Slightly Soluble
Phosphate buffer pH 6.8	18.74 ± 0.62	Sparingly Soluble
Phosphate buffer pH 7.4	14.53 ± 0.47	Sparingly Soluble
Methanol	483.60 ± 8.12	Freely Soluble
Acetone	52.37 ± 1.84	Soluble
Ethanol	78.42 ± 2.09	Soluble
DMSO	612.45 ± 9.73	Freely Soluble

Values are expressed in mean ± SD, (n=3)

FTIR analysis

The FTIR spectra of pure Aprepitant and its physical mixture with Kollidon® VA64 and Crospovidone XL-10 are shown in Fig. 2, along with their peak assignments. The FTIR spectrum of pure Aprepitant showed all characteristic absorptions of functional groups, such as N–H/O–H stretch at 3365.05 $cm^{-}1$, aromatic C–H stretch at 3110.10 $cm^{-}1$, aliphatic C-H stretch at 2980.00 cm−1 and C=O stretch (lactam/amide) at 1703.23 $cm^{-}1$. Distinct C–F stretching absorptions were present at 1510.46 cm^{-1} and 1154.76 cm^{-1}, which is typical for the trifluoromethyl groups in Aprepitant's structure. All major absorption bands of Aprepitant were present in the spectrum of the physical mixture with minor differences in their wavenumber values (N-H/O-H at 3370.00 cm^{-1}, C=O at 1701.07 cm^{-1}, and C-F at 1509.00 cm^{-1} and 1157.14 cm^{-1}, respectively). The physical mixture did not show any new peak formation or merging of bands into a broad band, as well as disappearance of peaks, revealing no chemical interaction between Aprepitant and the excipients. Preservation of all

characteristic peaks in the near-original positions indicated a good physicochemical compatibility of Aprepitant with selected excipients, Kollidon® VA64 and Crospovidone XL-10, and confirmed the suitability of this excipient mix for further formulation.

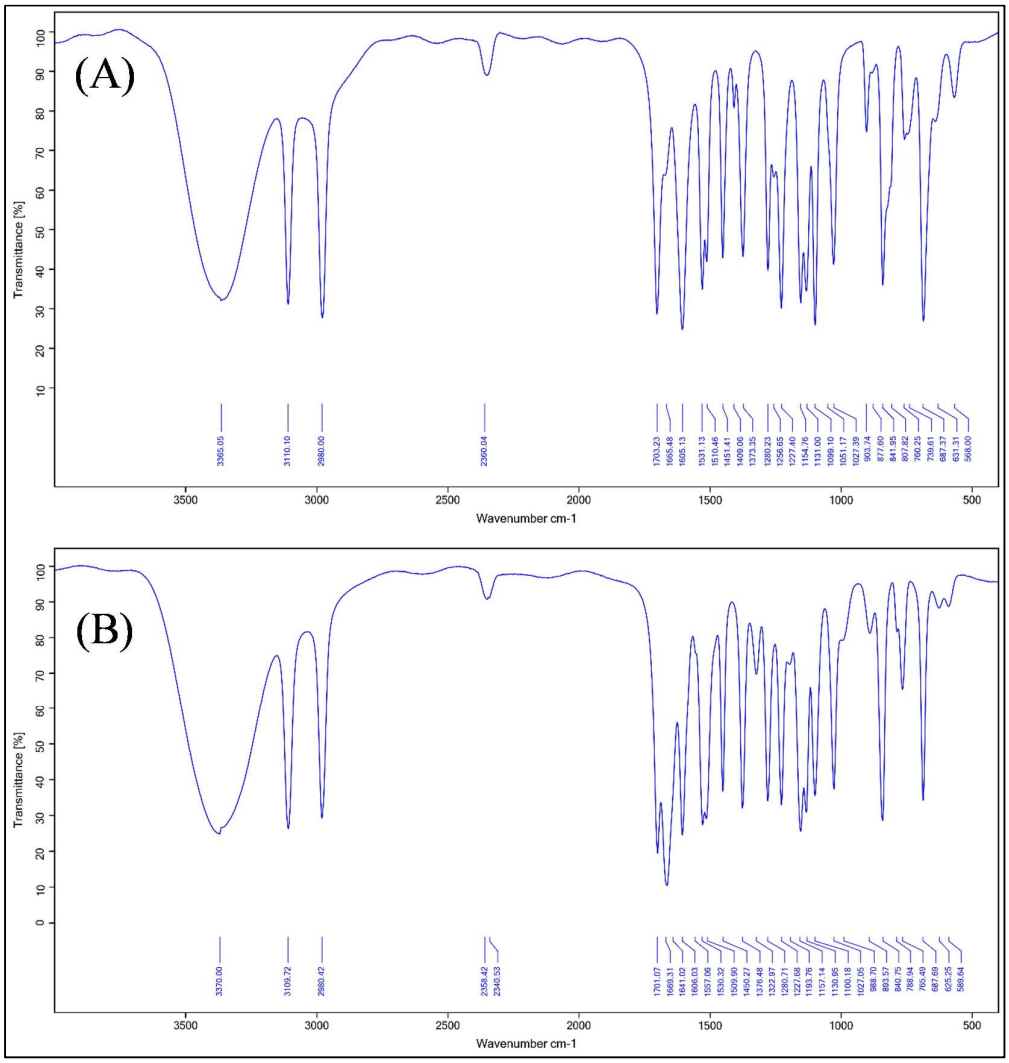

Figure 2: FTIR spectrum of (A) pure Aprepitant and (B) physical mixture of Aprepitant with Kollidon® VA64 and Crospovidone XL-10

DSC Analysis

Pure Aprepitant exhibited a distinct melting endotherm at 254.06 °C (onset: 250.81 °C; ΔH: −149.69 J/g), confirming its crystalline form and polymorphic purity, which is in agreement with the reported melting point of 254-256 °C (Fig. 3A). The physical mixture thermogram (Fig. 3B) revealed two endothermic peaks at 146.06 °C (ΔH: −26.10 J/g) and 159.58 °C (ΔH: −29.95 J/g) corresponding to the melting of Kollidon® VA64 and Crospovidone XL-10, respectively. The lack of Aprepitant's melting endotherm in the physical mixture indicated partial amorphization or molecular dispersion of the drug within excipients. No exothermic transitions were observed, indicating thermal stability of the mixture.

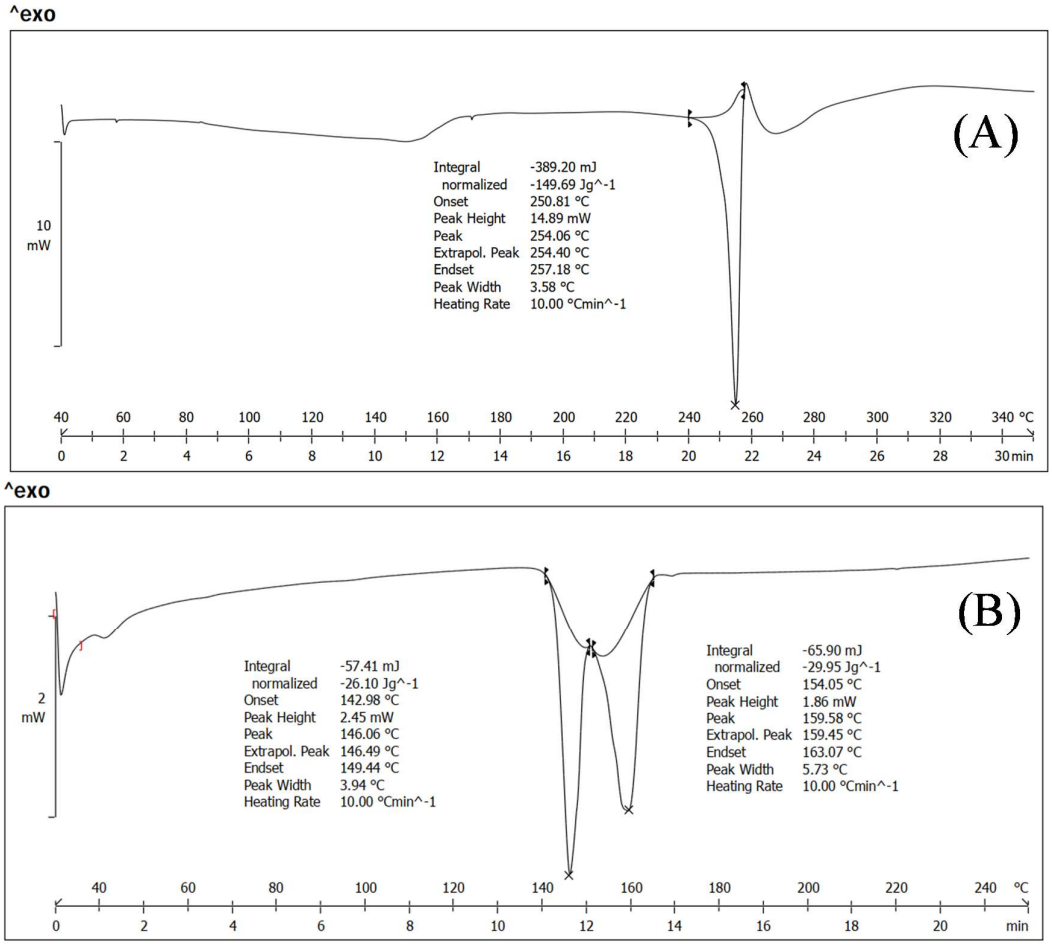

Figure 3: DSC thermogram of (A) pure Aprepitant and (B) physical mixture

Characterization of Aprepitant MDTs

The pre-compression properties of all nine powder mixtures (KF1 to KF9) are shown in Table 4. The angle of repose for all nine powder blends ranged from 25.4 ± 0.6° (KF9) to 27.4 ± 0.6° (KF1), all of which are lower than 30 degrees, suggesting good to excellent flow properties of all formulations. Bulk density values ranged between 0.412 ± 0.008 g/mL (KF1) and 0.431 ± 0.008 g/mL (KF9), while tapped density ranged from 0.476 ± 0.009 g/mL to 0.494 ± 0.009 g/mL across the same formulations. The Carr's index for all the formulations ranged between 12.75 ± 0.38% and 13.44 ± 0.42%, which indicated good compressibility according to the classification system. Hausner's ratio values ranged between 1.146 ± 0.013 (KF1) and 1.155 ± 0.012 (KF9), within the acceptable range of ≤ 1.25, further suggesting good flow characteristics of powder blends. An improvement in flow and compressibility indices was observed with increasing excipient concentrations from KF1 to KF9, but remained within acceptable limits.

Table 5 shows the post-compression evaluation results for KF1-KF9. Tablets were observed as white, flat-faced tablets with uniform thickness (3.20 ± 0.05 mm to 3.24 ± 0.05 mm) and diameter of about 10.01-10.02 mm in all batches due to the same tooling and compression parameters. Tablet hardness ranged from 3.26 ± 0.19 kg/cm² (KF9) to 3.47 ± 0.20 kg/cm² (KF7) with all batches demonstrating friability values less than 1% (KF9: 0.49 ± 0.03% and KF7: 0.65 ± 0.05%), showing good mechanical strength. Tablet weight variation for all formulations was in the range 299.4 ± 1.8 mg - 300.6 ± 1.9 mg (within ± 5% of IP/USP limits) and drug content varied from 98.37 ± 0.83% to 99.47 ± 0.61%, suggesting uniform distribution of drug throughout the tablet. The wetting time decreased progressively from 48.3 ± 1.6 sec (KF1) to 27.4 ± 1.1 sec (KF9), with a corresponding increase in water absorption ratio from 62.4 ± 2.3% to 84.6 ± 2.8%, respectively, due to increasing levels of Kollidon® VA64 and Crospovidone XL-10. The surface pH of all batches ranged between 6.72 ± 0.08 and 6.78 ± 0.07, well within the physiologically tolerable range (6.5-7.5), suggesting negligible risk of irritation to oral mucosa. In vitro dispersion time was found to decrease from 52.6 ± 2.1 sec (KF1) to 29.8 ± 1.4 sec (KF9), with the fastest dispersion observed for KF9 batches, in line with its highest water absorption ratio and lowest wetting time.

Table 4. Pre-compression evaluation of powder blends for Aprepitant MDTs (KF1–KF9)

Parameter	KF1	KF2	KF3	KF4	KF5	KF6	KF7	KF8	KF9
Angle of repose (°)	27.4 ± 0.6	26.8 ± 0.5	26.2 ± 0.7	27.1 ± 0.6	26.5 ± 0.5	25.9 ± 0.6	26.8 ± 0.7	26.1 ± 0.5	25.4 ± 0.6
Bulk density (g/mL)	0.412 ± 0.008	0.418 ± 0.007	0.424 ± 0.009	0.415 ± 0.007	0.421 ± 0.008	0.427 ± 0.007	0.417 ± 0.008	0.423 ± 0.009	0.431 ± 0.008
Tapped density (g/mL)	0.476 ± 0.009	0.481 ± 0.008	0.486 ± 0.010	0.478 ± 0.009	0.484 ± 0.008	0.490 ± 0.009	0.480 ± 0.010	0.487 ± 0.008	0.494 ± 0.009
Carr's index (%)	13.44 ± 0.42	13.10 ± 0.38	12.76 ± 0.45	13.18 ± 0.41	12.98 ± 0.39	12.86 ± 0.43	13.12 ± 0.44	13.14 ± 0.40	12.75 ± 0.38
Hausner's ratio	1.155 ± 0.012	1.150 ± 0.010	1.146 ± 0.013	1.152 ± 0.011	1.149 ± 0.010	1.148 ± 0.012	1.151 ± 0.013	1.152 ± 0.011	1.147 ± 0.010

Values are expressed as mean ± SD, (n=3)

Table 5: Post-compression evaluation parameters of Aprepitant MDTs (KF1–KF9).

Parameter	KF1	KF2	KF3	KF4	KF5	KF6	KF7	KF8	KF9
Appearance	White, flat-faced tablet	White, flat-faced tablet	White, flat-faced tablet	White, flat-faced tablet	White, flat-faced tablet	White, flat-faced tablet	White, flat-faced tablet	White, flat-faced tablet	White, flat-faced tablet
Thickness (mm)	3.21 ± 0.04	3.23 ± 0.03	3.24 ± 0.05	3.22 ± 0.04	3.21 ± 0.03	3.23 ± 0.04	3.20 ± 0.05	3.22 ± 0.03	3.24 ± 0.04
Diameter (mm)	10.01 ± 0.02	10.02 ± 0.03	10.01 ± 0.02	10.02 ± 0.03	10.01 ± 0.02	10.02 ± 0.02	10.01 ± 0.03	10.02 ± 0.02	10.01 ± 0.02
Hardness (kg/cm²)	3.42 ± 0.18	3.38 ± 0.21	3.31 ± 0.17	3.45 ± 0.19	3.36 ± 0.22	3.29 ± 0.16	3.47 ± 0.20	3.33 ± 0.18	3.26 ± 0.19
Friability (%)	0.61 ± 0.04	0.58 ± 0.03	0.54 ± 0.05	0.63 ± 0.04	0.57 ± 0.03	0.52 ± 0.04	0.65 ± 0.05	0.56 ± 0.04	0.49 ± 0.03
Weight variation (mg)	299.4 ± 1.8	300.2 ± 2.1	299.8 ± 1.6	300.6 ± 1.9	299.7 ± 2.0	300.1 ± 1.7	299.5 ± 1.8	300.3 ± 2.2	299.9 ± 1.6
Drug content (%)	98.42 ± 0.74	98.86 ± 0.81	99.12 ± 0.68	98.54 ± 0.79	99.03 ± 0.72	99.31 ± 0.65	98.37 ± 0.83	98.94 ± 0.70	99.47 ± 0.61
Wetting time (sec)	48.3 ± 1.6	41.7 ± 1.4	35.2 ± 1.3	43.6 ± 1.5	37.4 ± 1.2	31.8 ± 1.4	38.9 ± 1.7	33.1 ± 1.3	27.4 ± 1.1
Water absorption ratio (%)	62.4 ± 2.3	68.7 ± 2.1	74.3 ± 2.6	66.8 ± 2.4	72.5 ± 2.2	79.1 ± 2.5	70.3 ± 2.7	76.8 ± 2.3	84.6 ± 2.8
Surface pH	6.72 ± 0.08	6.74 ± 0.06	6.76 ± 0.07	6.73 ± 0.09	6.75 ± 0.07	6.77 ± 0.08	6.74 ± 0.06	6.76 ± 0.09	6.78 ± 0.07
In vitro dispersion time (sec)	52.6 ± 2.1	45.3 ± 1.8	38.7 ± 1.6	47.2 ± 2.0	40.8 ± 1.7	34.1 ± 1.5	42.4 ± 1.9	36.2 ± 1.6	29.8 ± 1.4

Values are expressed as mean ± SD, (n=3)

Cumulative percentage in vitro drug release

The in vitro drug release profiles of Aprepitant MDTs (KF1-9) in PBS pH 6.8 at 37 ± 0.5 °C are shown in Fig. 4. The order of drug release was consistent across all time points, with KF9 consistently showing the fastest release and KF1 the slowest, over the 45-minute experiment duration. After 2 minutes, drug release varied between 18.4 ± 1.2% (KF1) and 36.5 ± 1.8% (KF9), suggesting an early burst release effect. At 10 minutes, KF9 had released 81.4 ± 2.4% of the drug while KF1 had released 52.3 ± 1.8%, indicating that the concentration of excipients has a significant impact on the early release characteristics of the drug. By 15 minutes, the drug release ranged from 68.7 ± 2.1% (KF1) to 93.4 ± 2.6% (KF9), with formulations with higher concentrations of both Kollidon® VA64 and Crospovidone XL-10 showing higher drug release. Similarly, at 20 and 30 minutes, KF9 showed 97.1 ± 2.7% and 98.7 ± 2.8% release, whereas KF1 achieved only 77.2 ± 2.3% and 86.4 ± 2.4% release, respectively. At 45 minutes, all formulations reached drug release greater than 92% with KF9 showing near-complete drug release of 99.3 ± 2.9% and KF1 releasing 92.6 ± 2.6%. This gradual increase in drug release from KF1 to KF9 highlighted a positive correlation between the concentration of the solubilising carrier and superdisintegrant and improved dissolution, as visually observed in the release profiles in Fig. 4.

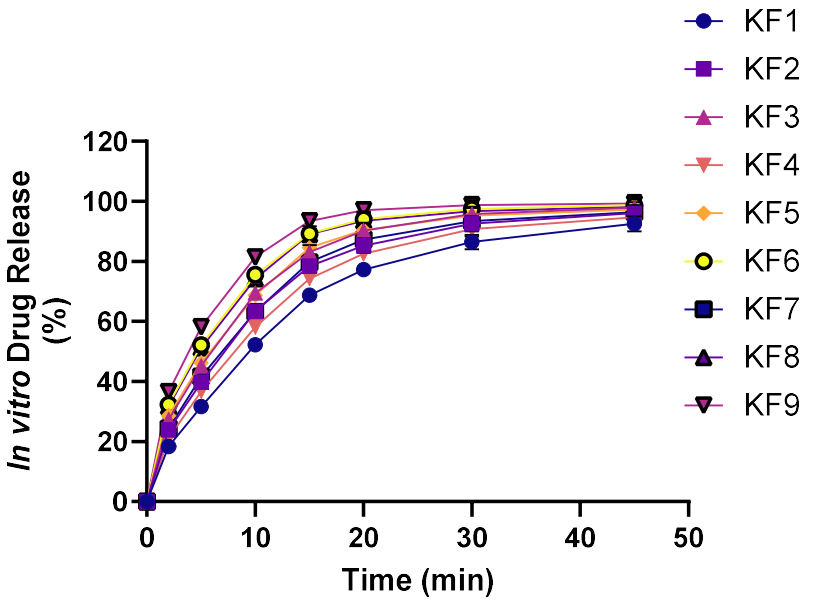

Figure 4. Cumulative percentage *in vitro* drug release (%) of Aprepitant MDTs KF1–KF9 in PBS pH 6.8 at 37 ± 0.5 °C, 50 rpm.

Table 6. Factorial design response data showing quadratic response pattern for Y1: disintegration time and Y2: cumulative drug release at 15 min (Q_{15}) for Aprepitant MDTs KF1–KF9.

Batch	X1: Kollidon® VA64 (mg)	X2: Crospovidone XL-10 (mg)	Y1: Disintegration Time (sec)	Y2: Q_{15} (%)
KF1	10 (-1)	4 (-1)	74.3 ± 2.4	68.7 ± 2.1
KF2	20 (0)	4 (-1)	58.6 ± 2.1	78.4 ± 2.3
KF3	30 (+1)	4 (-1)	52.4 ± 1.9	83.1 ± 2.4
KF4	10 (-1)	8 (0)	63.7 ± 2.2	74.2 ± 2.2
KF5	20 (0)	8 (0)	46.2 ± 1.8	84.6 ± 2.3
KF6	30 (+1)	8 (0)	41.8 ± 1.6	89.3 ± 2.5
KF7	10 (-1)	12 (+1)	57.4 ± 2.0	79.8 ± 2.3
KF8	20 (0)	12 (+1)	40.3 ± 1.7	89.1 ± 2.4
KF9	30 (+1)	12 (+1)	37.2 ± 1.4	93.4 ± 2.6

Values are expressed as mean ± SD, (n=3)

Optimization of Aprepitant Mouth Dissolving Tablets

Effect of variables on Disintegration Time (Y_1)

The Design-Expert fit summary statistic for disintegration time (Y_1) is shown in Table 7. The quadratic model was chosen from the models tested due to a sequential p-value of 0.0035, adjusted R^2 of 0.9953, and predicted R^2 of 0.9791. The adjusted and predicted R^2 values were close to each other and within the acceptable range (0.2), indicating good agreement. While the linear model was significant (sequential p = 0.0005), it had an adjusted R^2 and predicted R^2 of 0.8966 and 0.8341, respectively, suggesting a lack of fit to the curvature in the response. The two-factor interaction model had a sequential p-value of 0.8509, suggesting little gain over the linear fit. The cubic model was aliased and has not been considered due to a lack of degrees of freedom.

The results of the ANOVA for the quadratic model (Table 8) showed that the model was significant (F = 337.01, p = 0.0003). The largest contribution to Y_1 was made individually by factor A (Kollidon® VA64) with an F-value of 961.13 ($p < 0.0001$) and factor B (Crospovidone XL-10) with an F-value of 596.05 (p = 0.0002). The linear terms thus had a strong and significant effect on disintegration time. The quadratic terms A^2 (F = 104.78, p = 0.0020) and B^2 (F = 22.08, p = 0.0182) were also significant, suggesting the presence of curvature in the trend of the response within the experimental region. The interaction term AB (F = 1.02, p = 0.3875) was not significant, suggesting that the effects of the two factors on Y_1 were independent. The adequacy of the model was confirmed by the R^2 (0.9982), an adequate precision of 55.42, and a low coefficient of variation of 1.61%, indicating high signal-to-noise ratio and high

reproducibility of the experiment. The polynomial equation for Y_1 was:

$$Y_1 = 46.50 - 10.67A - 8.40B + 0.425AB + 6.10A^2 + 2.80B^2 \quad \ldots (1)$$

The negative signs of A (-10.67) and B (-8.40) coefficients showed that the increase in concentration of Kollidon® VA64 and Crospovidone XL-10, respectively, decreased disintegration time. The larger absolute value of the coefficient associated with A compared to that of B suggested a greater effect of Kollidon® VA64 on Y_1. The positive coefficients for the quadratic terms (A^2 (+6.10), B^2 (+2.80)) indicated an upward parabolic curve, implying that after reaching a certain concentration, increasing the concentration of either excipient resulted in a deceleration in the rate of reduction in disintegration time. The contour plots (Fig. 5A) and response surfaces (Fig. 5B) (two-dimensional and three-dimensional plots, respectively) illustrated this relationship. The elliptical contours of the contour plot converged towards lower disintegration time at increasing levels of both variables. The response surface showed the smooth curved decrease of Y_1 with increasing levels of both variables, with the largest gradient along the A-axis, as predicted by the largest coefficient in the regression equation.

Effect of variables on In vitro Drug Release at 15 min (Y_2)

The results for in vitro drug release at 15 min (Y_2) are shown in Table 7. The quadratic model was determined to be the best fit, with a sequential p-value of 0.0054, an adjusted R^2 of 0.9975 and predicted R^2 of 0.9893. The absolute difference between the two R^2 values of 0.0082 confirmed the suitability of the model to predict the release within the concentration range. The linear model, although significant (sequential $p < 0.0001$), had an adjusted R^2 of 0.9595 and a predicted R^2 of 0.9365, which were high but not sufficient to describe the response behaviour. The two-factor interaction model did not significantly improve the fit (sequential $p = 0.8260$), and the cubic model was aliased and so was removed from consideration.

The ANOVA table for the quadratic model of Y_2 (Table 8) indicated significant model fit ($F = 650.03$, $p < 0.0001$). Factor A (Kollidon® VA64) was the most influential term, recording an F-value of 2028.94 ($p < 0.0001$), followed by factor B (Crospovidone XL-10) with an F-value of 1125.45 ($p < 0.0001$). Thus the linear terms were extremely significant in drug release. The quadratic term A^2 ($F = 89.74$, $p = 0.0025$) reached statistical significance, while B^2 ($F = 4.98$, $p = 0.1117$) and the interaction term AB ($F = 1.05$, $p = 0.3812$) did not. The high R^2 (0.9991), adequate precision (78.59) and low coefficient of variation (0.47%) ensured a good fit of the model, with low experimental variation. The regression equation for Y_2 was:

$$Y_2 = 84.44 + 7.18A + 5.35B - 0.20AB - 2.62A^2 - 0.62B^2 \quad \ldots (2)$$

The positive coefficients for A (+7.18) and B (+5.35) indicated that increasing amounts of Kollidon® VA64 and Crospovidone XL-10 respectively, resulted in increasing in vitro drug release at 15 min. The magnitude of the coefficient for A was again greater, confirming its greater influence over factor B on Y_2. The negative coefficient for A^2 (−2.62), suggested a plateau effect at higher concentrations of Kollidon® VA64, where the improvement in drug release slowed down. In contrast, the coefficient for B^2 (−0.62) was relatively low and not statistically significant, implying a linear response between Crospovidone XL-10 concentration and Y_2, within the range investigated. The contour and response surface plots in Fig. 5C and 5D depicted these effects. The contour plot clearly showed a gradual shift towards higher drug release values with increasing concentrations of both variables, with a steeper slope along the A-axis. The 3D response surface showed a plateauing effect at high Kollidon® VA64 concentrations, consistent with the negative coefficient for the quadratic term in the regression equation, and also confirmed a more or less linear increase in Y_2 with increasing Crospovidone XL-10 concentration.

Table 7. Fit summary of the 3^2 full factorial design for disintegration time (Y_1) and in vitro drug release at 15 min (Y_2) responses.

Model	Sequential *p*-value	Lack of Fit *p*-value	Adjusted R^2	Predicted R^2	Remark
Response Y_1: Disintegration Time					
Linear	0.0005	-	0.8966	0.8341	
2FI	0.8509	-	0.8769	0.6236	
Quadratic	0.0035	-	0.9953	0.9791	**Suggested**
Cubic	0.3083	-	0.9986	0.9692	Aliased
Response Y_2: In vitro drug release at 15 min					
Linear	< 0.0001	-	0.9595	0.9365	
2FI	0.8260	-	0.9519	0.8706	
Quadratic	0.0054	-	0.9975	0.9893	**Suggested**
Cubic	0.3449	-	0.9991	0.9800	Aliased

2FI: Two-factor interaction; - : Not applicable for the respective model type.

Table 8. Analysis of variance (ANOVA) for the quadratic regression models of disintegration time (Y_1) and in vitro drug release at 15 min (Y_2) with corresponding fit statistics.

Source	Sum of Squares	df	Mean Square	*F*-value	*p*-value	Significance
Response Y_1: Disintegration Time						
Model	1196.85	5	239.37	337.01	0.0003	Significant
A – Kollidon® VA64	682.67	1	682.67	961.13	< 0.0001	
B – Crospovidone XL-10	423.36	1	423.36	596.05	0.0002	
AB	0.7225	1	0.7225	1.02	0.3875	
A^2	74.42	1	74.42	104.78	0.0020	
B^2	15.68	1	15.68	22.08	0.0182	
Residual	2.13	3	0.7103	-	-	
Cor Total	1198.98	8	-	-	-	
Response Y_2: In vitro drug release at 15 min						
Model	495.95	5	99.19	650.03	< 0.0001	Significant
A – Kollidon® VA64	309.60	1	309.60	2028.94	< 0.0001	
B – Crospovidone XL-10	171.74	1	171.74	1125.45	< 0.0001	
AB	0.1600	1	0.1600	1.05	0.3812	
A^2	13.69	1	13.69	89.74	0.0025	
B^2	0.7606	1	0.7606	4.98	0.1117	
Residual	0.4578	3	0.1526	-	-	
Cor Total	496.41	8	-	-	-	

df: degrees of freedom; C.V.: coefficient of variation; Adeq. Precision: adequate precision; Cor Total: corrected total; —: not applicable. $p < 0.05$ considered statistically significant.

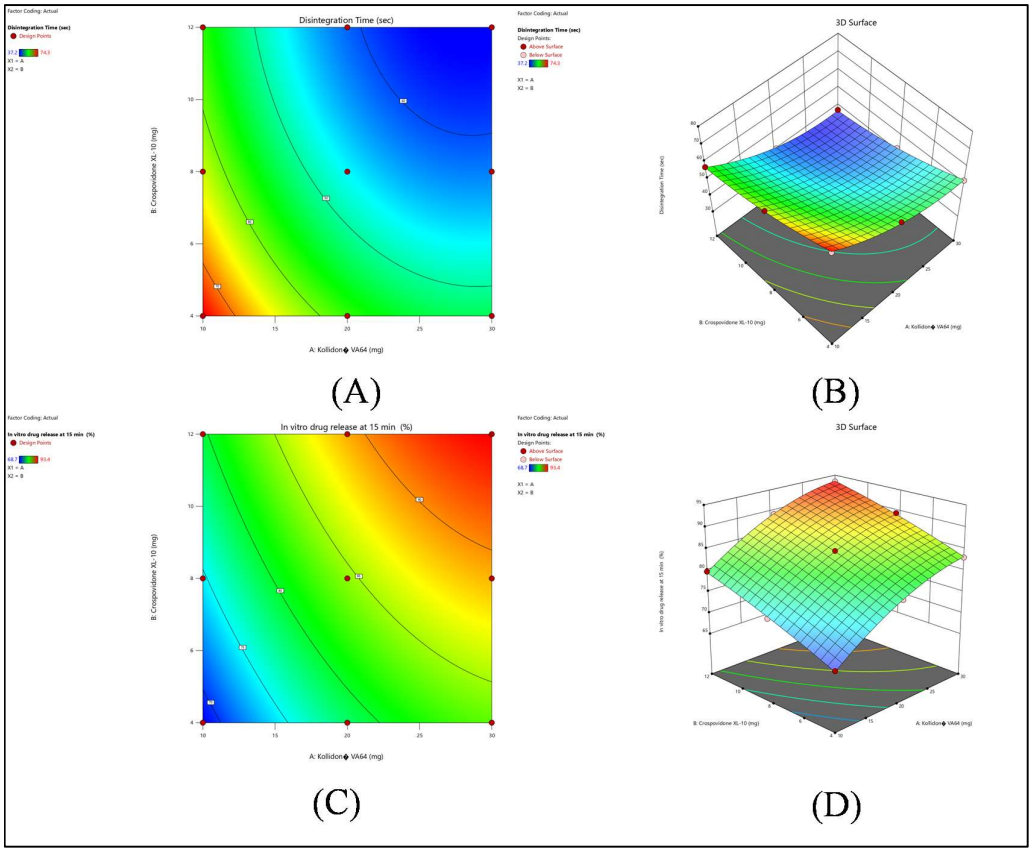

Figure 5. Influence of Kollidon® VA64 (A) and Crospovidone XL-10 (B) concentrations on critical quality attributes of Aprepitant mouth dissolving tablets. (A) Two-dimensional contour plot and (B) three-dimensional response surface plot illustrating the combined effect of independent variables on disintegration time (Y_1); (C) two-dimensional contour plot and (D) three-dimensional response surface plot depicting the combined effect on in vitro drug release at 15 min (Y_2).

Validation of statistical model

Validation of the optimized formulation (KF9) showed a good correlation between predicted and observed values, which validated the statistical model (Table 8). The predicted disintegration time (36.76 seconds) was found to be very close to the observed value (37.2 ± 1.4 seconds) with a very low bias of 1.19%. Likewise, the predicted drug release at 15 minutes (93.54%) was very similar to the actual value of 93.4 ± 2.6%, with a bias of 0.15%. The desirability value (1.000) also shows that the optimum formulation achieves the desired criteria. In conclusion, the close agreement between the predicted and observed results confirms the validity of the model.

Table 9. Statistical model validation: comparison of experimental and predicted values for optimized batch KF9

Parameter	Kollidon® VA64 (mg)	Crospovidone XL-10 (mg)	Disintegration Time (sec)	Q_{15} (%)	Desirability
Predicted	30	12	36.76	93.54	1.000
Experimental	30	12	37.2 ± 1.4	93.4 ± 2.6	-
% Bias	-	-	1.19	0.15	-

Accelerated Stability studies

The accelerated stability data for the optimized Aprepitant MDT formulation (batch KF9) stored at 40 ± 2 °C / 75 ± 5% RH for 90 days as per ICH Q1A(R2) guidelines are shown in Table 10. Visual observations of the tablets showed no change in appearance, with no discolouration, cracks or erosion of the surface at any stage of the study. Hardness increased slightly from 3.26 ± 0.19 kg/cm² to 3.31 ± 0.20 kg/cm², while friability increased from 0.49 ± 0.03% to 0.54 ± 0.04%, both of which are within the pharmacopoeial limits. Weight variation and drug content remained essentially unchanged over 90 days, with drug content at 90 days at 98.63 ± 0.74% versus initial drug content of 99.47 ± 0.61%, suggesting good chemical stability. Disintegration time increased modestly from 37.2 ± 1.4 sec to 39.4 ± 1.7 sec, and wetting time from 27.4 ± 1.1 sec to 29.1 ± 1.4 sec, while water absorption ratio declined marginally from 84.6 ± 2.8% to 83.2 ± 2.9%. Drug release at 15 min (Q_{15}) and 45 min showed no appreciable change, with 92.3 ± 2.9% and 98.5 ± 3.0% respectively at 90 days, compared to 93.4 ± 2.6% and 99.3 ± 2.9% at the initial time point, confirming that dissolution performance was unaffected by accelerated storage conditions.

Table 10. Accelerated stability study results of optimized Aprepitant MDT batch KF9 at 40 ± 2 °C / 75 ± 5% RH for 90 days.

Parameter	Initial (0 days)	30 days	60 days	90 days
Appearance	White, flat-faced tablet, no defects	White, flat-faced tablet, no defects	White, flat-faced tablet, no defects	White, flat-faced tablet, no defects
Hardness (kg/cm²)	3.26 ± 0.19	3.28 ± 0.21	3.29 ± 0.18	3.31 ± 0.20
Friability (%)	0.49 ± 0.03	0.51 ± 0.04	0.52 ± 0.03	0.54 ± 0.04
Weight variation (mg)	299.9 ± 1.6	300.1 ± 1.8	300.2 ± 1.7	300.4 ± 1.9
Drug content (%)	99.47 ± 0.61	99.21 ± 0.68	98.94 ± 0.72	98.63 ± 0.74
Disintegration time (sec)	37.2 ± 1.4	38.1 ± 1.6	38.7 ± 1.5	39.4 ± 1.7
Wetting time (sec)	27.4 ± 1.1	28.2 ± 1.3	28.6 ± 1.2	29.1 ± 1.4
Water absorption ratio (%)	84.6 ± 2.8	84.1 ± 2.6	83.7 ± 2.7	83.2 ± 2.9
Surface pH	6.78 ± 0.07	6.77 ± 0.08	6.76 ± 0.07	6.74 ± 0.09
Q_{15} (%)	93.4 ± 2.6	93.1 ± 2.7	92.7 ± 2.8	92.3 ± 2.9
Drug release at 45 min (%)	99.3 ± 2.9	99.1 ± 2.8	98.8 ± 2.9	98.5 ± 3.0

Values are expressed as mean ± SD, (n=3)

DISCUSSION

The study has been designed to develop and optimize mouth dissolving tablets of Aprepitant, a BCS Class IV NK_1 receptor antagonist with low solubility and dissolution rate limited oral bioavailability. The preformulation studies provided the physical properties of the drug and its suitability for MDT formulation. The drug's solubility (Table 3) indicated that Aprepitant solubility was found to be 4.18 ± 0.21 µg/mL in distilled water and 18.74 ± 0.62 µg/mL in PBS pH 6.8, reflecting its hydrophobicity and BCS Class IV status [41,42]. These results are in agreement with previous reports on Aprepitant's solubility, which have recorded a solubility of less than 20 µg/mL in water across physiological pH values [43]. FTIR spectra (Fig. 2) showed

that all the characteristic functional group absorptions of Aprepitant were retained in the physical mixture, with no new peaks or major shifts in peak position (beyond slight wavenumber shifts), confirmed drug-polymer (Kollidon® VA64 and Crospovidone XL-10) compatibility. DSC analysis (Fig. 3) showed the loss of Aprepitant's sharp endothermic melting peak at 254.06 °C in the physical mixture, indicative of partial conversion to an amorphous form and molecular interaction with the matrix [44]. This behaviour has been reported by Vasconcelos et al. in drug-polymer physical mixtures containing Kollidon® VA64, where the loss of crystallinity was explained by the formation of hydrogen bonds between the drug and the vinyl pyrrolidone-vinyl acetate backbone of the polymer, justifying the choice of Kollidon® VA64 as the main carrier in this formulation [45].

Pre-compression analysis (Table 4) demonstrated that all powder blends had acceptable flow and compressibility with Carr's index values of 12.75-13.44% and Hausner's ratio values of 1.146-1.155. formulations containing Kollidon® VA64 and superdisintegrants invariably resulted in powder blends with acceptable flow indices for direct compression. Post-compression indices (Table 5) were satisfactory with all batches, having drug content values between 98.37% and 99.47% and friability less than 1% for all formulations [46]. The gradual decrease in wetting time (48.3 sec for KF1 to 27.4 sec for KF9) and corresponding increase in water absorption ratio (62.4% to 84.6%) were in line with the increasing amounts of Crospovidone XL-10, which is known to be an efficient superdisintegrant due to capillary action. Similarly, Mohanachandran et al. found that the wetting time was significantly decreased and the water uptake was enhanced as the concentration of superdisintegrant increased in MDT formulations, consistent with the values observed in this study [47].

The optimization using a 3^2 full factorial design showed that the best fitting model was quadratic (Table 7) for both responses, with R^2 values of 0.9982 and 0.9991 for Y_1 and Y_2 respectively, signifying high predictability of the model. ANOVA (Table 8) further revealed that Kollidon® VA64 was the main factor affecting disintegration time (F=961.13) and in vitro drug release at 15 min (F=2028.94), followed by Crospovidone XL-10. These trends are reflected in the response surface plots (Fig. 1), with KF9 identified as the optimal formulation with a disintegration time of 37.2 sec and Q_{15} of 93.4 ± 2.6% [48]. These findings are consistent with the results of MDT formulations of poorly soluble drugs reported by Pahwa et al., in which Kollidon® VA64-based formulations consistently showed faster disintegration and higher early drug release in comparison to the conventional tablet systems. In vitro drug release profiles (Fig. 4) also showed that KF9 formulations released 99.3 ± 2.9% at 45 min, significantly higher than formulations with lower concentrations of excipients such as KF1 (92.6 ± 2.6%), confirming the concentration-dependent improvement in dissolution performance [49].

Accelerated stability testing at 40 ± 2 °C / 75 ± 5% RH for 90 days (Table 10) confirmed that the optimal KF9 formulation maintained its physical attributes, drug content (98.63 ± 0.74% at 90 days), and drug release (Q_{15} = 92.3 ± 2.9% at 90 days) over time, with all critical quality attributes (CQAs) within pharmacopoeial specifications. These observations are in line with stability studies of Kollidon® VA64-based oral solid dose forms, in which the moisture- and amorphous-stabilising properties of the polymer have been reported to maintain drug release performance under humid conditions [50]. But there are some limitations to the present study. The in vitro drug release experiments were carried out only in PBS at pH 6.8 and do not mimic the changing pH encountered in the gastrointestinal tract after oral dosing. The in vitro dissolution improvement of Aprepitant MDTs following formulation optimization was not evaluated in vivo in appropriate animal models and therefore may not translate to improved bioavailability. Moreover, the formulation was optimized using only two independent variables within a 3^2 factorial design, and the effects of other potentially significant factors like binder type, tablet compression force, and tablet coating have not been investigated. These issues should be explored in future studies by performing dissolution testing in biorelevant media, in vivo pharmacokinetic studies and a broader design space to better understand the performance of Aprepitant MDTs [51].

CONCLUSION

The current research successfully established and optimized Aprepitant mouth dissolving tablets through a 3^2 full factorial design considering Kollidon® VA64 and Crospovidone XL-10 as key formulation factors. Compatibility studies of all ingredients were successfully conducted and a series of optimization experiments identified KF9 as the formulation with the best critical quality attributes, disintegration time of 37.2 sec, Q_{15} of 93.4%, and almost complete drug release (99.3%) in 45 min. Stability studies of the optimized formulation over 90 days at accelerated conditions showed no considerable changes in physical and chemical attributes. The fast disintegration and improved dissolution of KF9 are of significant clinical importance for cancer patients suffering from dysphagia or chemotherapy-induced nausea and vomiting, in whom the conventional oral formulations are not well tolerated. These encouraging in vitro results need to be further validated on the basis of biorelevant dissolution and in vivo pharmacokinetic studies to confirm enhancement in bioavailability and development of a meaningful in vitro-in in vivo correlation.

Abbreviations

ANOVA: Analysis of Variance; BCS: Biopharmaceutics Classification System; CINV: Chemotherapy-Induced Nausea and Vomiting; C.V.: Coefficient of Variation; DSC: Differential Scanning Calorimetry; DMSO: Dimethyl Sulfoxide; df: Degrees of Freedom; FTIR: Fourier-Transform Infrared Spectroscopy; ICH: International Council for Harmonisation; IP: Indian Pharmacopoeia; MDT: Mouth Dissolving Tablet; MW: Molecular Weight; NK_1: Neurokinin-1; NF: National Formulary; PBS: Phosphate Buffer Saline; Q_{15}: Cumulative Drug Release at

15 Minutes; R^2: Coefficient of Determination; RH: Relative Humidity; SD: Standard Deviation; USP: United States Pharmacopoeia; UV: Ultraviolet Spectroscopy; 2FI: Two-Factor Interaction; ΔH: Enthalpy of Fusion; λmax: Maximum Absorption Wavelength.

Acknowledgements
The authors express sincere gratitude to the principal of the institute for providing the necessary laboratory infrastructure and research facilities that made this work possible. The authors also gratefully acknowledge Sciquaint Innovations Private Limited, Pune, India, for the sample of Aprepitant drug and for providing essential chemicals, technical support, and resources throughout the course of this study. The support extended by both institutions contributed significantly to the successful completion of this research work.

REFERENCES

1. Luo X, Yang L, Chen J, Zhang J, Zhao Q, Zhu J. Chemotherapy induced nausea and vomiting may cause anxiety and depression in the family caregivers of patients with cancer. Front Psychiatry 2023;14. https://doi.org/10.3389/fpsyt.2023.1221262.
2. Gautam S, Sharma KK, Amanat M. Management of Chemotherapy Induced Nausea Vomiting (CINV) in Breast Cancer Patients: An Imperative Factor in Patient Compliance. J Radiol Nurs 2023;42:315–20. https://doi.org/10.1016/j.jradnu.2023.04.002.
3. Ullah I, Ayaz M. A re-consideration of neural/receptor mechanisms in chemotherapy-induced nausea and vomiting: current scenario and future perspective. Pharmacol Rep 2023;75:1126–37. https://doi.org/10.1007/s43440-023-00514-z.
4. Gala D, Wright HH, Zigori B, Marshall S, Crichton M. Dietary strategies for chemotherapy-induced nausea and vomiting: A systematic review. Clin Nutr 2022;41:2147–55. https://doi.org/10.1016/j.clnu.2022.08.003.
5. Cheng J, Xu J, Shi R, Zhu W, Lu M, Mao Y. Chemotherapy-induced nausea and vomiting symptom experience in patients with non-small-cell lung cancer: A qualitative study. Medicine (Baltimore) 2025;104:e45097. https://doi.org/10.1097/MD.0000000000045097.
6. D'Amico F, Kelleher E, D'Andria Ursoleo J, Yavorovskiy AG, Turi S, Zaffaroni S, et al. The effect of Neurokinin-1 receptor antagonists on postoperative pain: A meta-analysis of randomized controlled trials. J Clin Anesth 2025;102:111772. https://doi.org/10.1016/j.jclinane.2025.111772.
7. Rodríguez FD, Coveñas R. The Neurokinin-1 Receptor: Structure Dynamics and Signaling. Receptors 2022;1:54–71. https://doi.org/10.3390/receptors1010004.
8. Rodríguez FD, Coveñas R. Association of Neurokinin-1 Receptor Signaling Pathways with Cancer. Curr Med Chem 2024;31:6460–86. https://doi.org/10.2174/0929867331666230818110812.
9. Borse LB, Bendale AR, Borse SL, Naphade VD, Jadhav AG. Formulation and Evaluation of Mouth Dissolving Tablet Rivaroxaban and its Validation. Biosci Biotechnol Res Asia 2022;19:943–54. https://doi.org/10.13005/bbra/3043.
10. Maharaj MK, Kumar A, Shafi T, Malik SH. Mouth-Dissolving Films: A Novel Approach for Oral Drug Delivery in Diabetic Management. Curr Pharm Res 2025:231–7. https://doi.org/10.63785/cpr.2025.1.2.193199.
11. Sharma R, Singh V, Ahuja M. Esterified guar gum: synthesis, characterization, and evaluation as excipient for mouth dissolving tablets. Int J Polym Anal Charact 2026;31:251–73. https://doi.org/10.1080/1023666X.2025.2561954.
12. Subramanian LS, Gayathri R, Karthikeyan, Dhivyadharshini R, Subramanian S. Nano formulation and evaluation of atorvastatin mouth dissolving tablets. Res J Pharm Technol 2024;17:1679–84.
13. Abdelhameed AH, Abdelhafez WA, Saleh kh I, Hamad AA, Mohamed MS. Formulation and optimization of oral fast dissolving films loaded with nanosuspension to enhance the oral bioavailability of Fexofenadine HCL. J Drug Deliv Sci Technol 2023;85:104578. https://doi.org/10.1016/j.jddst.2023.104578.
14. Elsayed MMA, Aboelez MO, Elsadek BEM, Sarhan HA, Khaled KA, Belal A, et al. Tolmetin Sodium Fast Dissolving Tablets for Rheumatoid Arthritis Treatment: Preparation and Optimization Using Box-Behnken Design and Response Surface Methodology. Pharmaceutics 2022;14:880. https://doi.org/10.3390/pharmaceutics14040880.
15. Mankar SD, Satpute A, Siddheshwar SS, Bhawar SB, Dighe SB. DESIGN, DEVELOPMENT AND OPTIMIZATION OF MOUTH DISSOLVING TABLET OF AMBRISENTAN USING DESIGN EXPERT SOFTWARE. Int J Appl Pharm 2023:282–90. https://doi.org/10.22159/ijap.2023v15i4.36398.
16. Husain M, Agnihotri VV, Goyal SN, Agrawal YO. Development, optimization and characterization of hydrocolloid based mouth dissolving film of Telmisartan for the treatment of hypertension. Food Hydrocoll Health 2022;2:100064. https://doi.org/10.1016/j.fhfh.2022.100064.
17. Patel SK, Prathyusha S, Kasturi M, Godse KC, Singh R, Rathi S, et al. Optimizing Irbesartan Fast

Dissolving Tablets Using Natural Polysaccharides for Enhanced Drug Delivery and Patient Compliance. Int Res J Multidiscip Scope 2025;06:1181–90. https://doi.org/10.47857/irjms.2025.v06i01.02542.

18. Rahimpour E, Moradi M, Sheikhi-Sovari A, Rezaei H, Rezaei H, Jouyban-Gharamaleki V, et al. Comparative Drug Solubility Studies Using Shake-Flask Versus a Laser-Based Robotic Method. AAPS PharmSciTech 2023;24:207. https://doi.org/10.1208/s12249-023-02667-9.
19. Farghaly DA, Afifi SA, Aboelwafa AA, Mohamed MI. Oral Dissolving Film of Rivastigmine: Optimization Using Factorial Design. J Pharm Innov 2023;18:1892–907. https://doi.org/10.1007/s12247-023-09743-4.
20. Ejeta F, Gabriel T, Joseph NM, Belete A. Formulation, Optimization and In Vitro Evaluation of Fast Disintegrating Tablets of Salbutamol Sulphate using a Combination of Superdisintegrant and Subliming Agent. Curr Drug Deliv 2022;19:129–41. https://doi.org/10.2174/1567201818666210614094646.
21. Vemula SK, Daravath B, Repka M. Quality by design (QbD) approach to develop fast-dissolving tablets using melt-dispersion paired with surface-adsorption method: formulation and pharmacokinetics of flurbiprofen melt-dispersion granules. Drug Deliv Transl Res 2023;13:3204–22. https://doi.org/10.1007/s13346-023-01382-z.
22. Sowjanya JN, Rao PR. Development, optimization, and invitro evaluation of novel fast dissolving oral films (FDOF's) of Uncaria tomentosa extract to treat osteoarthritis. Heliyon 2023;9. https://doi.org/10.1016/j.heliyon.2023.e14292.
23. Ibrahim AH, Ibrahim HM, Elbahwy IA, Afouna MI, Tagami T, Ozeki T. Lyophilized tablets of felodipine-loaded polymeric nanocapsules to enhance aqueous solubility: Formulation and optimization. J Drug Deliv Sci Technol 2022;70:103172. https://doi.org/10.1016/j.jddst.2022.103172.
24. Mohamed MS, El-Shenawy AA, Ramadan AE hakim, Mahmoud EA, Amin MA, Mohammed HA, et al. Metolazone co-crystals-loaded oral fast dissolving films: Design, optimization, and in vivo evaluation. J Drug Deliv Sci Technol 2023;90:105167. https://doi.org/10.1016/j.jddst.2023.105167.
25. Suksaeree J, Monton C, Charoenchai L, Chankana N, Wunnakup T. Optimization of Process and Formulation Variables for Semha–Pinas Extract Effervescent Tablets Using the Box–Behnken Design. AAPS PharmSciTech 2023;24:52. https://doi.org/10.1208/s12249-023-02514-x.
26. Özyılmaz ED, Comoglu T. Development of pediatric orally disintegrating mini-tablets containing atomoxetine hydrochloride-β-cyclodextrin inclusion complex using experimental design. Drug Dev Ind Pharm 2022;48:667–81. https://doi.org/10.1080/03639045.2022.2154787.
27. BASU B, MANKAD A, DUTTA A. Methylphenidate Fast Dissolving Films: Development, Optimization Using Simplex Centroid Design and In Vitro Characterization. Turk J Pharm Sci 2022;19:251–66. https://doi.org/10.4274/tjps.galenos.2021.99223.
28. Farooqui P, Gude R. FORMULATION DEVELOPMENT AND OPTIMISATION OF FAST DISSOLVING BUCCAL FILMS LOADED GLIMEPIRIDE SOLID DISPERSION WITH ENHANCED DISSOLUTION PROFILE USING CENTRAL COMPOSITE DESIGN. Int J Pharm Pharm Sci 2023:35–54. https://doi.org/10.22159/ijpps.2023v15i6.47992.
29. Almotairi N, Mahrous GM, Al-suwayeh S, Kazi M. Design and Optimization of Lornoxicam Dispersible Tablets Using Quality by Design (QbD) Approach. Pharmaceuticals 2022;15:1463. https://doi.org/10.3390/ph15121463.
30. Momeni M, Afkanpour M, Rakhshani S, Mehrabian A, Tabesh H. A prediction model based on artificial intelligence techniques for disintegration time and hardness of fast disintegrating tablets in pre-formulation tests. BMC Med Inform Decis Mak 2024;24:88. https://doi.org/10.1186/s12911-024-02485-4.
31. Alburyhi MM, Saif AA, Noman MA. FORMULATION AND EVALUATION OF BISOPROLOL FAST DISSOLVING TABLETS n.d.;12.
32. Ali SA, Alhakamy NA, Hosny KM, Alfayez E, Bukhary DM, Safhi AY, et al. Rapid oral transmucosal delivery of zaleplon–lavender oil utilizing self-nanoemulsifying lyophilized tablets technology: development, optimization and pharmacokinetic evaluation. Drug Deliv 2022;29:2773–83. https://doi.org/10.1080/10717544.2022.2115165.
33. Momeni M, Rakhshani S, Abbaspour M, Alizadeh F, Sheikhi N, GhorbanZadeh F, et al. Dataset development of pre-formulation tests on fast disintegrating tablets (FDT): data aggregation. BMC Res Notes 2023;16:131. https://doi.org/10.1186/s13104-023-06416-w.

34. Alalaiwe A, Alsenaidy MA, Almalki ZS, Fayed MH. Development and Optimization of Sildenafil Orodispersible Mini-Tablets (ODMTs) for Treatment of Pediatric Pulmonary Hypertension Using Response Surface Methodology. Pharmaceutics 2023;15:923. https://doi.org/10.3390/pharmaceutics15030923.
35. Izzalddin RS, Hussein NR, Ramadhan SA, Taher MO, Younis SA, Omer HK, et al. Development and Characterization of Fast-Dissolving Tablets for the Combination Therapy of Ketorolac and Rizatriptan Benzoate. J Pharm Innov 2025;20:235. https://doi.org/10.1007/s12247-025-10156-8.
36. Somadasan S, Subramaniyan G, Athisayaraj MS, Sukumaran SK. Central Composite Design: An Optimization Tool for Developing Pharmaceutical Formulations. J Young Pharm 2024;16:400–9. https://doi.org/10.5530/jyp.2024.16.52.
37. Raykar M, Velraj M. DESIGN, DEVELOPMENT AND EVALUATION OF NOVEL MOUTH DISSOLVING FILM OF TOFACITINIB CITRATE. Int J Appl Pharm 2023:324–32. https://doi.org/10.22159/ijap.2023v15i1.46064.
38. Elmowafy M, Alruwaili NK, Ahmad N, Kassem AM, Ibrahim MF. Quercetin-Loaded Mesoporous Silica Nanoparticle–Based Lyophilized Tablets for Enhanced Physicochemical Features and Dissolution Rate: Formulation, Optimization, and In Vitro Evaluation. AAPS PharmSciTech 2022;24:6. https://doi.org/10.1208/s12249-022-02464-w.
39. Aswathy KN, Asdaq SMB, Saritha CK, Thomas L, Haridas N, Viswanad V, et al. Formulation and in-vitro characterization of fast-disintegrating herbal extract sublingual immunotherapy tablet for peanut-induced allergic asthma. Saudi J Biol Sci 2022;29:1283–97. https://doi.org/10.1016/j.sjbs.2021.12.031.
40. Kamali H, Farzadnia P, Movaffagh J, Abbaspour M. Optimization of curcumin nanofibers as fast dissolving oral films prepared by emulsion electrospinning via central composite design. J Drug Deliv Sci Technol 2022;75:103714. https://doi.org/10.1016/j.jddst.2022.103714.
41. Khan A, Majeedullah, Qayum M, Ahmad L, Ahmad Khan S, Abbas M. Optimization of diluents on the basis of SeDeM-ODT expert system for formulation development of ODTs of glimepiride. Adv Powder Technol 2022;33:103389. https://doi.org/10.1016/j.apt.2021.12.008.
42. Abla KK, Mneimneh AT, Allam AN, Mehanna MM. Application of Box-Behnken Design in the Preparation, Optimization, and In-Vivo Pharmacokinetic Evaluation of Oral Tadalafil-Loaded Niosomal Film. Pharmaceutics 2023;15:173. https://doi.org/10.3390/pharmaceutics15010173.
43. Shah KA, Gao B, Kamal R, Razzaq A, Qi S, Zhu Q-N, et al. Development and Characterizations of Pullulan and Maltodextrin-Based Oral Fast-Dissolving Films Employing a Box–Behnken Experimental Design. Materials 2022;15:3591. https://doi.org/10.3390/ma15103591.
44. Fouad SA, Teaima MH, Gebril MI, Abd Allah FI, El-Nabarawi MA, Elhabal SF. Formulation of novel niosomal repaglinide chewable tablets using coprocessed excipients: in vitro characterization, optimization and enhanced hypoglycemic activity in rats. Drug Deliv 2023;30:2181747. https://doi.org/10.1080/10717544.2023.2181747.
45. Sheta NM, Boshra SA, Mamdouh MA, Abdel-Haleem KM. Design and optimization of silymarin loaded in lyophilized fast melt tablets to attenuate lung toxicity induced via HgCl2 in rats. Drug Deliv 2022;29:1299–311. https://doi.org/10.1080/10717544.2022.2068696.
46. Fathy Elhabal S, El-Nabarawi MA, Abdelaal N, Elrefai MFM, Ghaffar SA, Khalifa MM, et al. Development of canagliflozin nanocrystals sublingual tablets in the presence of sodium caprate permeability enhancer: formulation optimization, characterization, in-vitro, in silico, and in-vivo study. Drug Deliv 2023;30:2241665. https://doi.org/10.1080/10717544.2023.2241665.
47. Sopyan I, Gozali D, Sriwidodo, Guntina RK. DESIGN-EXPERT SOFTWARE (DOE): AN APPLICATION TOOL FOR OPTIMIZATION IN PHARMACEUTICAL PREPARATIONS FORMULATION. Int J Appl Pharm 2022:55–63. https://doi.org/10.22159/ijap.2022v14i4.45144.
48. Nakamura S, Fukai T, Sakamoto T. Orally Disintegrating Tablet Manufacture via Direct Powder Compression Using Cellulose Nanofiber as a Functional Additive. AAPS PharmSciTech 2022;23:1. https://doi.org/10.1208/s12249-021-02194-5.
49. Naureen F, Shah Y, Shah SI, Abbas M, Rehman IU, Muhammad S, et al. Formulation Development of Mirtazapine Liquisolid Compacts: Optimization Using Central Composite Design. Molecules 2022;27:4005. https://doi.org/10.3390/molecules27134005.
50. Rassol ST, Qader AB. FORMULATION AND OPTIMIZATION OF DOMPERIDONE-LOADED LIQUID SNEDDS: CHARACTERIZATION AND IN-VITRO EVALUATION. Sci J Univ Zakho 2025;13:435–47. https://doi.org/10.25271/sjuoz.2025.13.3.1576.

51. Triboandas H, Pitt K, Bezerra M, Ach-Hubert D, Schlindwein W. Itraconazole Amorphous Solid Dispersion Tablets: Formulation and Compaction Process Optimization Using Quality by Design Principles and Tools. Pharmaceutics 2022;14:2398. https://doi.org/10.3390/pharmaceutics14112398.